SNAP Peas: What triggered star formation far off the Main Sequence?

Principal Investigator: Prof. Kevin Schawinski

Institution: Eidgenossiche Technische Hochschule (ETH)

Electronic Mail: kevin.schawinski@phys.ethz.ch

Scientific Category: UNRESOLVED STELLAR POPULATIONS AND GALAXY STRUCTURE

Scientific Keywords: Galaxy Formation And Evolution, Galaxy Morphology And Structure, High Redshift Galaxies, Interacting And Merging Galaxies

Instruments: WFC3

Number of targets: 71

Proprietary Period: 12

Abstract

The `green pea' galaxies, discovered by the Galaxy Zoo citizen scientists, are low-mass, low-metallicty starburst galaxies with star formation rates so high that they are a factor of 10-100 off the Main Sequence of star formation. Given the apparent universality of the Main Sequence and the rarity of significant outliers, the green peas will yield key insights into galaxy evolution. In many of their properties, the green peas are more like high redshift star forming galaxies and reside in low density environments, perhaps even in voids. Are they driven by an accretion mode analogous to the cold flows seen at high redshift? If so, the peas should resemble the turbulent disks with embedded clumps seen at z~2. They could also be triggered by mergers of galaxies with near-primordial gas. The peas are too faint and compact to observe from the ground, so we propose a SNAP survey of peas to study their morphology.

Investigators:

	Investigator	Institution	Country
PI*&	Prof. Kevin Schawinski	Eidgenossiche Technische Hochschule (ETH)	CHE
CoI#	Prof. Claudia Megan Urry	Yale University	USA/CT
CoI*	Dr. Karen Louise Masters	Portsmouth University/ICG	GBR
CoI*	Dr. Chris J. Lintott	University of Oxford	GBR
CoI*	Dr. Brooke Devlin Simmons	University of Oxford	GBR
CoI*	Dr. Oliver Hahn	Eidgenossiche Technische Hochschule (ETH)	CHE
CoI	Dr. Carolin Noel Cardamone	Brown University	USA/RI
CoI	Dr. William C. Keel	University of Alabama	USA/AL
CoI*	Dr. Steven Bamford	University of Nottingham	GBR
CoI	Dr. Kyle Willett	University of Minnesota - Twin Cities	USA/MN
CoI	Lucy Fortson	University of Minnesota - Twin Cities	USA/MN

Number of investigators: 11
* ESA investigators: 6
# US Admin CoI: Prof. Claudia Megan Urry
& Phase I contacts: 1

Target Summary:

Target	RA	Dec	Magnitude
587725576962244831	17 27 6.3295	+59 49 2.18	V = 19
587731513693503653	03 22 44.8997	+00 44 42.40	
587724233716596882	01 29 10.1518	+14 59 34.64	
587726032778559604	10 57 16.7280	+02 32 7.05	
587726032253419628	12 44 23.3717	+02 15 40.43	
588010360138367359	08 42 16.9512	+03 38 6.73	
587726102030451047	15 47 9.1051	+03 36 14.09	
587729155743875234	11 33 3.8035	+65 13 41.38	
587728919520608387	14 11 45.3374	+62 39 11.30	
587729229297090692	15 37 37.2742	+58 47 40.47	
587725818034913419	15 40 50.1934	+57 24 41.95	
587730774416883967	22 37 35.0594	+13 36 47.02	
587730774965354630	00 26 52.0764	+15 27 37.66	
587728906099687546	07 49 36.7716	+33 37 16.39	
587725550133444775	10 26 15.2100	+63 33 8.51	
588009371762098262	11 22 19.7338	+61 54 45.46	
588011122502336742	12 07 5.3141	+61 35 11.84	

Target	RA	Dec	Magnitude
588011103712706632	15 06 27.9881	+56 27 2.67	
587732134315425958	13 01 28.3224	+51 04 51.21	
587732152555864324	07 47 58.0037	+23 36 32.81	
587732578845786234	10 31 38.9314	+07 15 56.52	
587733080270569500	10 53 30.8234	+52 37 52.87	
588297864714387604	08 47 54.0854	+33 36 54.82	
587735695911747673	13 39 40.7117	+55 27 40.09	
587735696987717870	14 14 31.2089	+54 30 56.11	
587733441055359356	16 46 6.5381	+31 30 53.49	
588017605211390138	10 18 3.2441	+41 06 21.10	
588017114517536797	14 24 5.7283	+42 16 46.29	
588017116132540589	15 14 8.6364	+38 52 7.38	
588018090541842668	15 43 1.2259	+34 46 1.48	
588018090013098618	16 47 35.5351	+22 46 58.81	
588016878295515268	09 11 31.1518	+31 27 26.78	
587735661007863875	09 17 2.5270	+31 52 20.58	
588016892783820948	09 54 50.9590	+37 21 55.80	
587735663159738526	09 57 39.7723	+37 42 7.61	
588018055114784812	14 40 9.9406	+46 19 36.95	
588018055652769997	14 54 35.5850	+45 28 56.24	
588017570848768137	12 48 34.6344	+12 34 2.93	
587736915687964980	16 04 36.6643	+08 19 59.10	
587736915687375248	15 59 25.9778	+08 41 19.16	
587738410863493299	10 11 57.0840	+13 08 22.10	
587735349111947338	12 19 3.9838	+15 26 8.51	
587738570859413642	13 39 28.3039	+15 16 42.13	
587736940372361382	14 30 27.5093	+34 09 16.99	
587739153352229578	07 51 57.7834	+16 38 13.24	
587738947196944678	08 15 52.0030	+21 56 23.65	
587738371672178952	08 22 47.6616	+22 41 44.08	
588017978880950451	10 02 13.5586	+34 42 17.67	
587739408388980778	11 37 22.1398	+35 24 26.69	
588017977277874181	11 26 37.7645	+38 03 2.92	
587739406242742472	11 52 4.8845	+34 00 49.87	
587739828742389914	14 57 35.1372	+22 32 1.80	
587739652107600089	15 52 10.0015	+21 03 12.28	
587739721387409964	16 37 19.3034	+14 39 4.96	
587741600420003946	12 05 0.6737	+26 20 47.74	
587741421099286852	08 26 51.8071	+18 20 51.84	
587741532770074773	08 53 24.0850	+19 30 22.61	

Target	RA	Dec	Magnitude
587741817851084830	09 11 13.3447	+18 31 8.17	
587741391573287017	09 43 47.2214	+26 20 42.58	
587741392649781464	10 09 18.9962	+29 16 21.50	
587739648351076573	10 20 57.4627	+29 37 26.46	
587741490367889543	10 32 26.9573	+27 17 55.25	
587741532781215844	10 39 7.1664	+27 28 21.03	
587742014876745993	09 27 28.6769	+17 40 18.62	
588023240745943289	09 22 49.2689	+19 13 39.46	
587745243087372534	09 25 32.3671	+14 03 13.04	
587742628534026489	16 13 6.3161	+09 29 49.16	
587744874785145599	08 05 18.0418	+09 25 33.52	
587742013825941802	13 10 36.7394	+21 48 17.03	
587742062151467120	13 06 56.3530	+22 41 38.41	
587741727655919734	12 55 2.7158	+25 56 9.28	

Observing Summary:

Target	Config Mode and Spectral Elements	Flags	Orbits
587725576962244831	WFC3/UVIS Imaging F336W		1
	WFC3/UVIS Imaging F475W		
587731513693503653	WFC3/UVIS Imaging F336W		1
	WFC3/UVIS Imaging F475W		
587724233716596882	WFC3/UVIS Imaging F336W		1
	WFC3/UVIS Imaging F475W		
587726032778559604	WFC3/UVIS Imaging F336W		1
	WFC3/UVIS Imaging F475W		
587726032253419628	WFC3/UVIS Imaging F336W		1
	WFC3/UVIS Imaging F475W		
588010360138367359	WFC3/UVIS Imaging F336W		1
	WFC3/UVIS Imaging F475W		
587726102030451047	WFC3/UVIS Imaging F336W		1
	WFC3/UVIS Imaging F475W		
587729155743875234	WFC3/UVIS Imaging F336W		1
	WFC3/UVIS Imaging F475W		
587728919520608387	WFC3/UVIS Imaging F336W		1
	WFC3/UVIS Imaging F475W		
587729229297090692	WFC3/UVIS Imaging F336W		1

Target	Config Mode and Spectral Elements	Flags	Orbits
	WFC3/UVIS Imaging F475W		
587725818034913419	WFC3/UVIS Imaging F336W		1
	WFC3/UVIS Imaging F475W		
587730774416883967	WFC3/UVIS Imaging F336W		1
	WFC3/UVIS Imaging F475W		
587730774965354630	WFC3/UVIS Imaging F336W		1
	WFC3/UVIS Imaging F475W		
587728906099687546	WFC3/UVIS Imaging F336W		1
	WFC3/UVIS Imaging F475W		
587725550133444775	WFC3/UVIS Imaging F336W		1
	WFC3/UVIS Imaging F475W		
588009371762098262	WFC3/UVIS Imaging F336W		1
	WFC3/UVIS Imaging F475W		
588011122502336742	WFC3/UVIS Imaging F336W		1
	WFC3/UVIS Imaging F475W		
588011103712706632	WFC3/UVIS Imaging F336W		1
	WFC3/UVIS Imaging F475W		
587732134315425958	WFC3/UVIS Imaging F336W		1
	WFC3/UVIS Imaging F475W		
587732152555864324	WFC3/UVIS Imaging F336W		1
	WFC3/UVIS Imaging F475W		
587732578845786234	WFC3/UVIS Imaging F336W		1
	WFC3/UVIS Imaging F475W		
587733080270569500	WFC3/UVIS Imaging F336W		1
	WFC3/UVIS Imaging F475W		
588297864714387604	WFC3/UVIS Imaging F336W		1
	WFC3/UVIS Imaging F475W		
587735695911747673	WFC3/UVIS Imaging F336W		1
	WFC3/UVIS Imaging F475W		
587735696987717870	WFC3/UVIS Imaging F336W		1
	WFC3/UVIS Imaging F475W		
587733441055359356	WFC3/UVIS Imaging F336W		1
	WFC3/UVIS Imaging F475W		
588017605211390138	WFC3/UVIS Imaging F336W		1
	WFC3/UVIS Imaging F475W		
588017114517536797	WFC3/UVIS Imaging F336W		1
	WFC3/UVIS Imaging F475W		
588017116132540589	WFC3/UVIS Imaging F336W		1
	WFC3/UVIS Imaging F475W		
588018090541842668	WFC3/UVIS Imaging F336W		1

Target	Config Mode and Spectral Elements	Flags	Orbits
	WFC3/UVIS Imaging F475W		
588018090013098618	WFC3/UVIS Imaging F336W		1
	WFC3/UVIS Imaging F475W		
588016878295515268	WFC3/UVIS Imaging F336W		1
	WFC3/UVIS Imaging F475W		
587735661007863875	WFC3/UVIS Imaging F336W		1
	WFC3/UVIS Imaging F475W		
588016892783820948	WFC3/UVIS Imaging F336W		1
	WFC3/UVIS Imaging F475W		
587735663159738526	WFC3/UVIS Imaging F336W		1
	WFC3/UVIS Imaging F475W		
588018055114784812	WFC3/UVIS Imaging F336W		1
	WFC3/UVIS Imaging F475W		
588018055652769997	WFC3/UVIS Imaging F336W		1
	WFC3/UVIS Imaging F475W		
588017570848768137	WFC3/UVIS Imaging F336W		1
	WFC3/UVIS Imaging F475W		
587736915687964980	WFC3/UVIS Imaging F336W		1
	WFC3/UVIS Imaging F475W		
587736915687375248	WFC3/UVIS Imaging F336W		1
	WFC3/UVIS Imaging F475W		
587738410863493299	WFC3/UVIS Imaging F336W		1
	WFC3/UVIS Imaging F475W		
587735349111947338	WFC3/UVIS Imaging F336W		1
	WFC3/UVIS Imaging F475W		
587738570859413642	WFC3/UVIS Imaging F336W		1
	WFC3/UVIS Imaging F475W		
587736940372361382	WFC3/UVIS Imaging F336W		1
	WFC3/UVIS Imaging F475W		
587739153352229578	WFC3/UVIS Imaging F336W		1
	WFC3/UVIS Imaging F475W		
587738947196944678	WFC3/UVIS Imaging F336W		1
	WFC3/UVIS Imaging F475W		
587738371672178952	WFC3/UVIS Imaging F336W		1
	WFC3/UVIS Imaging F475W		
588017978880950451	WFC3/UVIS Imaging F336W		1
	WFC3/UVIS Imaging F475W		
587739408388980778	WFC3/UVIS Imaging F336W		1
	WFC3/UVIS Imaging F475W		
588017977277874181	WFC3/UVIS Imaging F336W		1

Target	Config Mode and Spectral Elements	Flags	Orbits
	WFC3/UVIS Imaging F475W		
587739406242742472	WFC3/UVIS Imaging F336W		1
	WFC3/UVIS Imaging F475W		
587739828742389914	WFC3/UVIS Imaging F336W		1
	WFC3/UVIS Imaging F475W		
587739652107600089	WFC3/UVIS Imaging F336W		1
	WFC3/UVIS Imaging F475W		
587739721387409964	WFC3/UVIS Imaging F336W		1
	WFC3/UVIS Imaging F475W		
587741600420003946	WFC3/UVIS Imaging F336W		1
	WFC3/UVIS Imaging F475W		
587741421099286852	WFC3/UVIS Imaging F336W		1
	WFC3/UVIS Imaging F475W		
587741532770074773	WFC3/UVIS Imaging F336W		1
	WFC3/UVIS Imaging F475W		
587741817851084830	WFC3/UVIS Imaging F336W		1
	WFC3/UVIS Imaging F475W		
587741391573287017	WFC3/UVIS Imaging F336W		1
	WFC3/UVIS Imaging F475W		
587741392649781464	WFC3/UVIS Imaging F336W		1
	WFC3/UVIS Imaging F475W		
587739648351076573	WFC3/UVIS Imaging F336W		1
	WFC3/UVIS Imaging F475W		
587741490367889543	WFC3/UVIS Imaging F336W		1
	WFC3/UVIS Imaging F475W		
587741532781215844	WFC3/UVIS Imaging F336W		1
	WFC3/UVIS Imaging F475W		
587742014876745993	WFC3/UVIS Imaging F336W		1
	WFC3/UVIS Imaging F475W		
588023240745943289	WFC3/UVIS Imaging F336W		1
	WFC3/UVIS Imaging F475W		
587745243087372534	WFC3/UVIS Imaging F336W		1
	WFC3/UVIS Imaging F475W		
587742628534026489	WFC3/UVIS Imaging F336W		1
	WFC3/UVIS Imaging F475W		
587744874785145599	WFC3/UVIS Imaging F336W		1
	WFC3/UVIS Imaging F475W		
587742013825941802	WFC3/UVIS Imaging F336W		1
	WFC3/UVIS Imaging F475W		
587742062151467120	WFC3/UVIS Imaging F336W		1

Target	Config Mode and Spectral Elements	Flags	Orbits
587741727655919734	WFC3/UVIS Imaging F475W WFC3/UVIS Imaging F336W WFC3/UVIS Imaging F475W		1

Total prime orbits: 71

- **Scientific Justification**

SNAP Peas: what is the nature of extremely star-forming galaxies in the local universe?

The "Green Peas" are true Living Fossils of the Early Universe

When the "Green Peas" were discovered by the citizen scientists taking part in the Galaxy Zoo project, we did not anticipate finding genuine living fossils in the SDSS data of nearby galaxies. First dubbed the "Peas" because of their compact, green appearance in the SDSS *gri* colour composite images, the Peas have been revealed to be *extraordinary, intense starbursts at z~0.3 unlike any others in the low redshift universe*. In many of their properties, they seem to belong to a much earlier epoch. As such, they can inform galaxy formation theory the same way living fossils such as coelacanths and tuataras shed light on biological evolution.

What can the Peas tell us about Star Formation in Galaxies?

The Galaxy Zoo citizen scientists quickly assembled a sample of unusual galaxiesPeas whose common properties were "small, round and green" [in the SDSS image, see Figure 1], hence the name "Peas". This Peas Corps collected the original sample and in collaboration with the Galaxy Zoo team scientists put together a publication announcing their discovery and describing their basic properties (Cardamone et al. 2009; C09 hereafter).

C09 refine their selection via SDSS broad-band colours. Peas have unusual *gri* colours away from stars, galaxies and quasars due to their extreme emission line spectra. The SDSS *r* band is so dominated by [OIII 5007] emission that they appear green in the SDSS colour map (*g*=blue, *r*=green, *i*=red). The spectra show extreme, low-metallicity starburst lines, with a small subsection of the Peas being narrow-line Seyfert 1 AGN.

The starburst Peas are extraordinary in many of their properties. Chief among them are their specific star formation rates. Star-forming galaxies exhibit a remarkably tight, near-linear relationship between galaxy mass and star formation rate (SFR), dubbed the "*main sequence of star formation*" (Brinchmann et al. 2004; Elbaz et al. 2007; Salim et al. 2007; Noeske et al. 2007; Peng et al. 2010; Elbaz et al. 2011). This relationship increases with redshift until reaching a plateau about a factor of ~20 higher at z~1, tracing the drop in cosmic star formation rate density since z~1. To put it another way, a star forming galaxy at high redshift would have a much higher total SFR than a galaxy at z~0 at the same stellar mass.

The Peas at z~0.3, seemingly unaware of this huge drop in typical specific star formation rate (SSFR=SFR/M) exhibit star formation rates of up to a factor of ~100 higher than main sequence starformers at z~0 (see Figure 2). Chemically, the Peas were first thought to be on the mass-metallicity relation, but it has since been shown by Amorin et al. (2010) that they are *below* the local mass-metallicity relation.

The Peas can thus be described as galaxies quite unlike any other in the nearby universe: they are forming stars more efficiently, are chemically less evolved, physically more concentrated than their main sequence cousins. In many ways, they resemble high redshift starformers.

The Peas are odd in other ways too: Chakraborti et al. (2012) use radio observations to show that they have strong magnetic fields of ~30μG, stronger than the Milky Way. The Peas are also unresolved at the SDSS resolution, limiting their half-light radii to less than ~5 kpc.

Cold Flows, Clumpy Disks, Voids and more

The mass function of haloes in voids is different from that in most of the rest of the universe (Hahn et al. 2007) with a characteristic M* that is lower. Perhaps, void central haloes are still below the critical halo mass at which gas accretion switches from cold flows to hot mode accretion (e.g. Dekel & Birnboim 2006, Cattaneo et al. 2006 Dekel et al. 2009), so these void haloes could still experience something analogous to the cold flows that fuel high redshift starbursts, albeit with some difference. The chief difference being the much lower mean density of the universe which would force any cold flows to `puff up'.

The similarity to high redshift galaxies makes them intriguing. There is some evidence from C09 and more recent analysis (see Figure 4) that the Peas reside in low density environments, and perhaps in voids.

High redshift star forming galaxies are thought to accrete baryons much more efficiently via these cold flows leading to the formation of compact, starforming galaxies with unstable disks prone to forming sub-clumps (e.g. Forster-Schreiber et al. 2009; Tacconi et al. 2010; Burkert et al. 2010). As the halo mass increases to $\sim 10^{12}$ Msun, these gas inflows start to shock at the Virial radius leading to significantly less inflow of gas to the central galaxy as the gas now has to cool down before becoming available for star formation. This leads to a drastic decrease in SSFR.

Could the Peas be a leftover of this cold mode of gas accretion? Is this why they lie so far off the main sequence? Why are the Peas so different from other star forming galaxies? As extreme outliers from a very tight relation such as the main sequence of star formation, the Peas demand an explanation, and any explanation will lead to key insights into galaxy evolution.

This Proposal: What do the Peas actually look like?

There are two possible explanations for the extraordinary properties of the Peas:

1. As argued above, the Peas could be fed by something analogous to a cold flow still active at low redshift in rare void galaxies. In this case, we would expect their morphology to be similar to that of typical high redshift star forming galaxies, namely they should resemble the clumpy, turbulent disk galaxies seen by e.g. Forster-Schreiber et al. (2009) Tacconi et al. (2010), or Burkert et al. (2010).

2. The main alternative is that the Peas are major mergers of void galaxies, perhaps bringing in significant amounts of near-pristine gas and triggering the first major episode of star formation in void galaxies.

Only Hubble has the imaging resolution to resolve the Peas and tell us whether they are mergers or clumpy, turbulent disk galaxies. As part of the investigation of basic properties by C09, archival images of 5 Peas were found (see Figure 3). All three star forming Peas (marked SB, top row) have an irregular appearance. While intriguing, a sample of 3 star forming Peas is insufficient to draw conclusions.

We therefore propose a SNAP survey of star forming Peas which will allow us to generate a sufficiently large sample to characterize the range of morphologies of Pea galaxies and evaluate the relative importance of major mergers and turbulent disks in driving their extraordinary star formation properties.

Team Expertise, Analysis Plan and Outreach

Our team has the expertise to rapidly reduce, analyze and publish the results from these observations. We plan to reduce and analyze the data as soon as it becomes available and publish them with a rapid turn-around time. Moreover, since the Peas were discovered by Galaxy Zoo citizen scientists, we plan to publicize the observations, analysis and publication of the results to the over quarter million Galaxy Zoo citizen scientists via social media (blog, Twitter, Facebook).

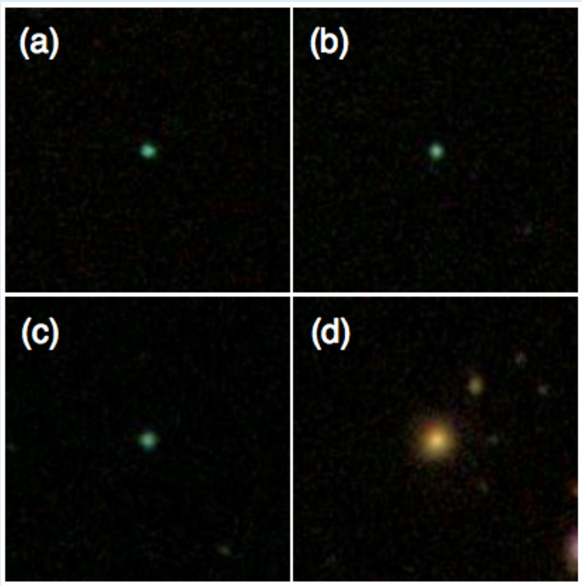

Figure 1: SDSS colour gri colour composites of three Peas (a,b,c) and a comparison galaxy at the same redshift (d). The Peas are unresolved at the SDSS imaging resolution (C09).

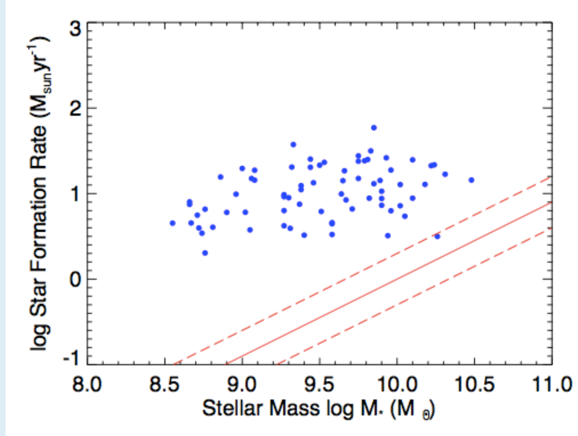

Figure 2: The z~0 main sequence and scatter (red lines) from Peng et al. (2012) and the Peas (blue points, C09). The Peas scatter far off the main sequence and have SFRs a factor of 10-100 higher than expected for their given stellar mass.

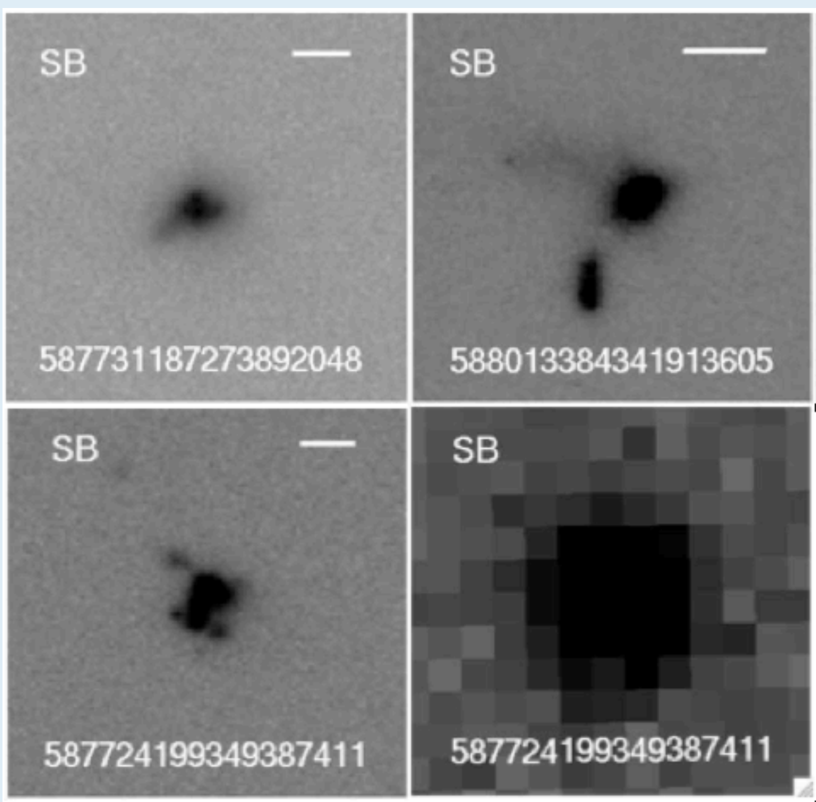

Figure 3: Existing *HST* images of star-forming Peas from the archive (presented inC09). The bottom right is the ground-based SDSS image of the star-forming pea to the left of it and on the same scale - showing that it is completely unresolved. The exposure times are 2200-3600 seconds.

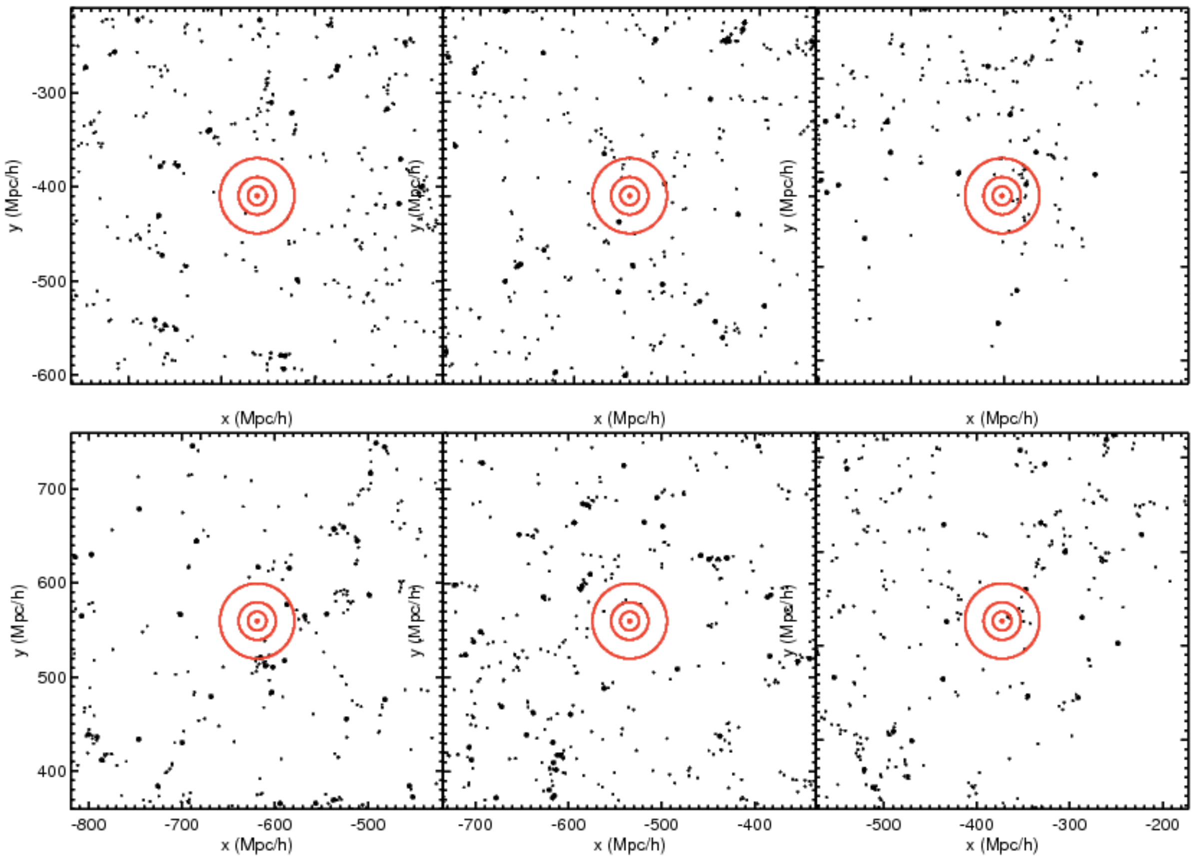

Figure 4: The environment of Pea galaxies. Each panel shows a star forming Pea (red point at the center) compared to neighboring LRGs from SDSS DR7 (from Kazin et al.) in comoving coordinates. The concentric red circles around the Peas indicate distances of 10, 20 and 40 Mpc/h. While LRGs are a very biased tracer of large scale structure, they are the only tracer available at 0.2<z<0.4. Peas avoid clusters and have a typical distance of ~15 Mpc/h to the nearest LRG (not accounting for biases due to Peas near survey edges). This, together with the low neighbor count presented by C09 indicates that Peas stronly prefer low density environments and likely live in voids.

- ## Description of the Observations

Sample Selection

The input sample for this SNAP proposal are the 73 Peas from C09 (minus those already in the archive) unambiguously identified as star forming. Assuming a completion rate comparable to SNAP programs from previous cycles, we estimate that 73*0.3 ≈ 22 Peas will be observed. 22 objects imply a Poisson noise of ~4.7, which means that even if the Peas are made up of two distinct categories by morphology, we will be able to statistically distinguish them.

Details of Observations

The Peas feature extremely strong emission lines that distort the broad-band SED shape. We therefore choose appropriate WFC3/UVIS filters to avoid the strong [OIII 5007], to image the stellar continuum on both sides of the 4000 Angstrom break. The combined filters will let us not just map the overall morphology, but also identify rough age gradients: clumps in gas-rich disks should be younger and therefore bluer. We also choose filters that are blue - the Peas are blue andUV-luminous and therefore easiest to observe there in short exposures.

We choose the F336W and F475W to span the 4000 A break, redshifted to z~0.3, where the Peas are. F475W avoids the [OIII] line, though may contain some of the bluer emission lines - these are sufficiently weak that they do not significantly distort the broad-band flux. As the blue filter, we choose F336W. Having this rest-frame UV filter will allow us to do basic measurements of age gradients across the peas and see if any of the supposed clumps are indeed bluer and younger.

Despite the inclusion of F336W, we do not choose to include this proposal as part of the "UV initiative" as the use of the UV filter is not essential, merely helpful.

We will naturally use the entire ~45 minutes of each SNAP orbit.

Simulations to Establish Sensitivity Limits

As we have archival *HST* observations of Peas (see Figure 3 and C09), we can in any case estimate that the imaging depths achieved in 1 orbit are more than sufficient to detect even faint features. Splitting the SNAP orbit time between two filters is therefore enough to reach the imaging depth required. The Peas range in *g*-band apparent magnitude from 18 to 20.5 AB, so we list them as V=19 in the target list.

References

Amorin et al., 2010, ApJL, 715, L128 • Burkert et al. 2010, ApJ, 725, 2324 • Brinchmann et al. 2004, MNRAS, 351, 1151 • Cardamone et al., 2009, MNRAS, 399, 1191 • Cattaneto et al., 2006, MNRAS, 370, 1651 • Chaktraborti et al. 2012, ApJL, 746, L6 • Dekel & Birnboim 2006, MNRAS, 368, 2 • Dekel et al. 2009, Nature, 457, 451 • Elbaz D. et al., 2007, A&A, 468, 33 • Elbaz D. et al., 2011, A&A, 533, A119 • Forster-Schreiber et al. 2009, ApJ, 706, 1364 • Kazin et al. 2010, ApJ, 710, 1444 • Noeske et al., 2007, ApJ, 660, L43 • Peng et al., 2010, ApJ, 721, 193 • Salim et al., 2007, ApJS, 173, 267 • Tacconi et al., 2010, Nature, 463, 781 •

- **Special Requirements**

  None.

- **Coordinated Observations**

  None.

- **Justify Duplications**

  None.

- **Past HST Usage**

The PI is not leading any recent *HST* proposals but he is a Co-I on the following recent programs:

Cycle 19, program 12525, PI Keel, “Giant Ionized Clouds Around Local AGN - Obscuration and History”, first observations taken in November 2011 and reduction/analysis in progress.

Cycle 19, program 12500, PI Kaviraj, “High-resolution UV studies of SAURON galaxies with WFC3: constraining recent star formation and its drivers in local early-type galaxies”, analysis in progress.

Cycle 17, program 11620, PI Keel, “A Quasar Light Echo in the Local Universe?”, results published in AJ.